Evaluation of intraocular lens position and retinal shape in negative dysphotopsia using high-resolution magnetic resonance imaging

Vught, L. van; Dekker, C.E.; Stoel, B.C.; Luyten, G.P.M.; Beenakker, J.W.M.

Open

ARTICLE

Evaluation of intraocular lens position and retinal shape in negative dysphotopsia using high-resolution magnetic resonance imaging

Luc van Vught, BSc, Cornelis E. Dekker, MSc, Berend C. Stoel, MSc, PhD, Gregorius P.M. Luyten, MD, PhD, FEBOphth, Jan-Willem M. Beenakker, MSc, PhD

Purpose: To assess potential relationships of intraocular lens (IOL) position and retinal shape in negative dysphotopsia (ND).

Setting: Department of Ophthalmology, Leiden University Medical Center, Leiden, the Netherlands.

Design: Case-control study.

Methods: High-resolution ocular magnetic resonance imaging (MRI) scans were performed in patients with ND and pseudophakic controls, and subsequently used to determine the displacement and tilt of the in-the-bag IOL about the pupil and iris. In addition, anterior segment tomography was used to assess the iris–IOL distance. Furthermore, the retinal shape was quantified from the MRI scans by fitting an ellipse to the segmented inner boundary of the retina. Both the IOL position and retinal shape were compared between groups to assess their potential role in the etiology of ND.

Results: In total, 37 patients with ND and 26 pseudophakic controls were included in the study. The mean displacement and tilt of the IOL were less than 0.1 mm and 0.5 degrees, respectively, in both groups and all directions. The corresponding mean iris–IOL distance was 1.1 mm in both groups. Neither of these values differed statistically significantly between groups (all *P* values >.6). The retinal shape showed large variations but was not statistically significantly different between the groups in both the left–right (*P* = .10) and the anterior–posterior (*P* = .56) directions.

Conclusions: In this study, the in-the-bag IOL position and retinal shape did not statistically significantly differ between patients with ND and the general pseudophakic population. Given the large variation in retinal shape between subjects, however, it could still be an important factor in a multifactorial origin of ND.

J Cataract Refract Surg 2021; 47:1032–1038

Negative dysphotopsia (ND) is a visual complaint that can occur after an otherwise uneventful cataract surgery and is generally described as a shadow or dark region in the far peripheral visual field that is mainly experienced under photopic conditions.[1,2] The incidence of ND is reported to be up to 19% directly after cataract surgery when actively asked.[3,4] Although it generally improves or fully disappears over time, 3.2% of patients are still experiencing complaints 1 year postoperatively, making additional treatment often necessary.[4] The treatments proposed for ND are mostly surgical and are generally aimed at affecting the path of light within the eye.[1,2,5–13] None of the proposed treatments have shown to fully resolve ND in all cases, and additional understanding of the exact origin of ND is required to fully resolve this condition. Many potential factors of influence have been proposed, including pupil size, angle κ, size of the capsular overlap, diffusiveness of the capsular bag, position of the intraocular lens (IOL) about the iris, design of the IOL, and extent of the functional nasal retina.[2,5,9,10,14–17]

For most of these factors, clinical validation based on evaluations of larger patient groups has not yet been reported. Recently, we combined multiple optical evaluations to establish clinical support for a smaller pupil size, a more temporally displaced pupil center, a stronger temporally tilted iris, and a difference in peripheral refraction in patients with ND compared with pseudophakic patients without complaints.[18] These optical measurements cannot,

Submitted: October 15, 2020 | Final revision submitted: December 2, 2020 | Accepted: December 26, 2020

From the Department of Ophthalmology, Leiden University Medical Center, Leiden, the Netherlands (van Vught, Luyten, Beenakker); Department of Radiology, C.J. Gorter Center for High Field MRI, Leiden University Medical Center, Leiden, the Netherlands (van Vught, Beenakker); Division of Image Processing (LKEB), Department of Radiology, Leiden University Medical Center, Leiden, the Netherlands (Dekker, Stoel).

Supported by the ESCRS, Co Dublin, Ireland; and Stichting Leids Oogheelkundig Ondersteuningsfonds, Oegstgeest, the Netherlands.

Presented at ISMRM Benelux, Arnhem, the Netherlands, January 2020 and 214e jaarvergadering van het Nederlands Oogheelkundig Gezelschap, Groningen, the Netherlands, Spetember 2020.

Corresponding author: Luc van Vught, BSc, Department of Ophthalmology, Leiden University Medical Center, Albinusdreef 2, 2333 ZA Leiden, the Netherlands. Email: l.van_vught@lumc.nl.

0886-3350/$ - see frontmatter
https://doi.org/10.1097/j.jcrs.0000000000000576

however, assess all the factors that are potentially involved in ND because visual inspection of part of the eye is prevented by the iris. For example, the IOL position cannot be accurately determined behind the natural, nonwidened, pupil. Furthermore, optical techniques are not able to evaluate the peripheral retinal shape, which could be a contributing factor to ND because it is experienced in the far peripheral field.

Magnetic resonance imaging (MRI) is, unlike conventional ophthalmic imaging modalities, in principle able to provide insight into a number of these factors because it is able to image the complete eye. MRI can, therefore, visualize the location of the IOL and the shape of the retina. Unfortunately, because high-resolution ocular MR images are generally affected by eye motion, the resolution of ocular MRI was too limited for detailed anatomical mapping of the retina and IOL.[19,20] Recent advances in MRI, such as ultra-high-field MRI, have, however, enabled the acquisition of high-resolution ocular MR images without increasing the acquisition time.[21,22] Furthermore, dedicated eye protocols have made the MR images acquisition less prone to eye motion–related artifacts that would otherwise prevent clinical interpretation.[22,23] Because of these advances, the complete eye can now be imaged with MRI with high accuracy.[24–26] In this study, we used these high-resolution MRI techniques to quantify both the in-the-bag position of the IOL and the retinal shape in the pseudophakic population to assess their potential relation with ND.

METHODS

Thirty-seven patients with ND and 26 pseudophakic controls with in-the-bag–implanted IOLs were prospectively studied at the Leiden University Medical Center as part of the ESCRS vRESPOND study (CCMO-registry number: NL58358.058.16). The study was performed in conformance with the tenets of the Declaration of Helsinki and approved by the local Medical Ethics Committee. The criteria for the diagnosis of ND consisted of a patient-reported shadow or dark region in the temporal peripheral visual field that occurred after an otherwise uneventful cataract surgery and the absence of any other evident cause of this visual complaint. Thirty-three (89%) of the 37 patients with ND actively reported ND-like complaints to their ophthalmologist after cataract surgery, whereas 4 (11%) patients with ND reported a temporal shadow on active screening in the context of a scientific study. In total, 28 (76%) of the 37 patients with ND were referred from other hospitals or clinics. Twenty-six pseudophakic controls were included from 3 different sites after reporting no temporal shadow on active screening at inclusion. One control was excluded during the study because the MR images revealed staphyloma. As a result, the final analyses were performed on 37 patients with ND and 25 pseudophakic controls.

For each subject, 1 eye was imaged on a 7-Tesla Philips Achieva MRI (Phillips) using a dedicated eye coil.[27] Two types of 3D MR images were acquired: a T1-weighted scan (3DT1) with a resolution of $0.45 \times 0.45 \times 0.90$ mm^3 and a T2-weighted scan (3DT2) with a resolution of $0.6 \times 0.6 \times 0.6$ mm^3 (Figure 1, A and B). A cued-blinking protocol was used to minimize ocular motion in both scans.[22,23] For subjects who had difficulty to adhere to the cued-blinking instructions, a faster scan with a slightly lower resolution of $0.75 \times 0.75 \times 0.75$ mm^3 that required no blinking was added. In addition, the eye was evaluated with the LENSTAR LS900 biometer (Haag-Streit AG) and the Pentacam anterior segment tomographer (OCULUS Optikgeräte GmbH).

The 3DT1 MRI scan was acquired with a gradient echo readout with an echo time of 2.5 milliseconds (ms), a repetition time of 4.9 ms, and a flip angle of 10 degrees. For the 3DT2 scan, the acquisition was performed using a turbo spin echo readout with an echo time of 254 ms, a repetition time of 2500 ms, and a refocusing angle of 35 degrees. The geometrical relationship between the iris and the IOL was assessed on the T1-weighted images because they had the highest resolution, whereas the retinal shape was evaluated on the T2-weighted images because of their increased contrast-to-noise ratio between the vitreous and retina.

To assess the alignment and tilt of the IOL about the pupil and iris on the MR images, dedicated software was in-house developed

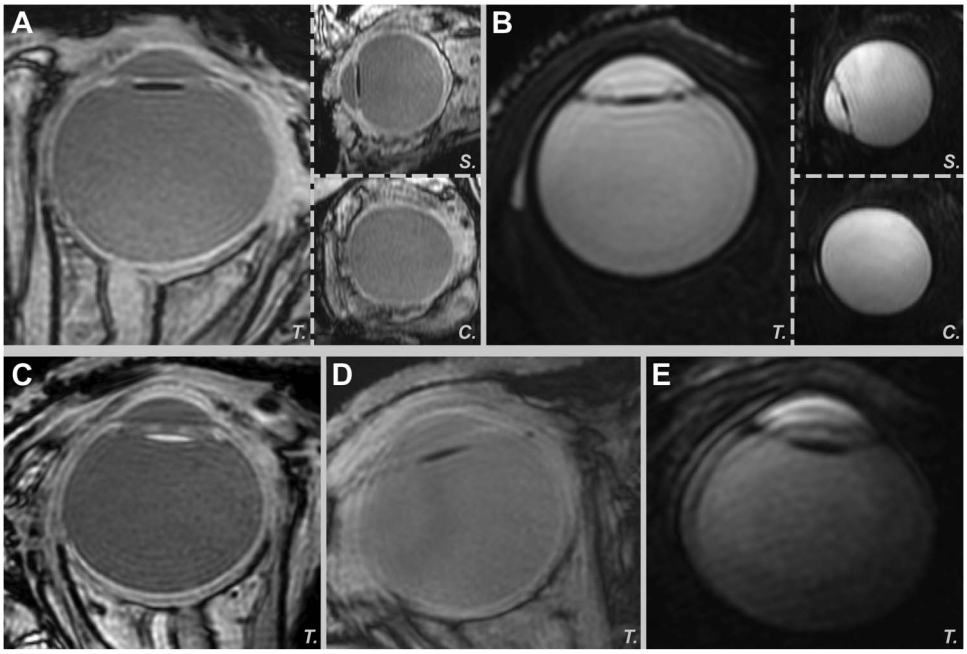

Figure 1. Examples of high-resolution 3D MRI scans. *A*: A 3DT1 scan with normal quality in transversal (*T.*) view, showing a hypointense IOL. The sagittal (*S.*) and coronal (*C.*) reconstructions are also shown. *B*: A 3DT2 scan with normal quality. *C*: A 3DT1 scan with normal quality and a hyperintense, hydrophilic, IOL. *D*: A 3DT1 scan with mild motion artifacts that required manual correction of the segmentation. *E*: A 3DT2 scan with movement artifacts that required the use of a scan with a slightly lower resolution that did not have cued-blinking motion control.

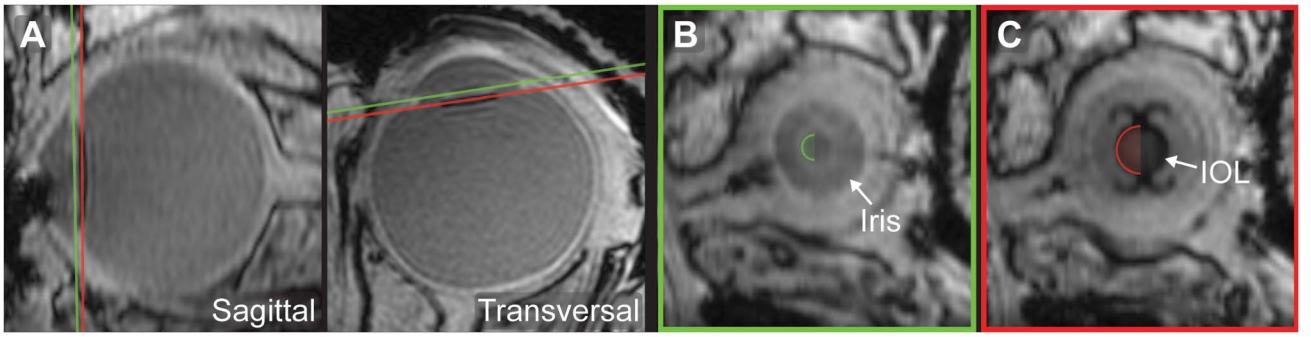

Figure 2. Example of the determination of the geometrical relation between the iris and the IOL using the 3DT1 MR images. *A*: The multiplanar reconstruction planes defined through the iris (*green line*) and through the IOL (*red line*) on sagittal and transversal views. *B*: The reconstructed image of the iris with a manual annotation of the pupil by a best-fit circle (*green semicircle*). *C*: The reconstructed view of the IOL with a manual annotation of the IOL optic by a best-fit circle (*red semicircle*).

in MeVisLab (version 3.0.2, MeVis Medical Solutions AG). Within this software, two 3D multiplanar reconstructions were created from the 3DT1 scans to accurately define the IOL and iris plane for each subject (Figure 2, A). On these multiplanar reconstructions, the pupil and IOL were annotated manually by a best-fit circle (Figure 2, B and C), after which their relative alignment and tilt in 3D were assessed in the horizontal and vertical directions. This procedure was fully repeated for the horizontal alignment in 15 randomly selected healthy controls to assess the reproducibility of the analysis. In addition, to assess the distance between the anterior surface of the iris and the IOL, a 2D plane was automatically fitted to the iris on the topography measurement as described previously, and the difference between the axial location of this plane and the anterior chamber depth (ACD) was calculated.[18] Because the Pentcam's ACD measurements are reported to be incorrect in some pseudophakic patients, the ACDs were measured manually on 3 different Scheimpflug images and subsequently averaged.[28]

The retinal shape was evaluated by automatically segmenting the inner boundary of the retina–sclera complex on the 3DT2 scan using 3D subdivision fitting in MeVisLab, providing a 3D shape of the vitreous body that includes posterior vitreous detachments if present (Figure 3, A).[24] The central axis of the eye was then defined as the line through the center of the vitreous body and the center of the manually annotated IOL (Figure 3, B). An ellipse was subsequently fitted through a horizontal cross-section of the retina by minimizing the orthogonal distance between the segmented retina and the ellipse, using the SciPy library in Python (version 3.6, Python Software Foundation) (Figure 3, B and C).[A] The degrees of freedom of the ellipse in the fitting process were limited to its left–right (LR) radius, its anterior–posterior (AP) radius, and the AP position of its center (Figure 3, C).

In the statistical analysis, the axial length and the geometrical relationship between the iris and IOL were compared between groups using Levene tests for the variation and unpaired *t* tests for the averages. Furthermore, the relation between axial length and retinal shape was assessed by calculating the Pearson correlation coefficient between the axial length and the radii of the fitted ellipse. Finally, the retinal shape, represented by the width and height of the fitted ellipse, was compared using an analysis of covariance test with the axial length as covariant. All statistical analyses were performed in IBM SPSS Statistics for Windows software (version 25, IBM Corp.) with an α value less than 0.05 as threshold for statistical significance.

RESULTS

The demographic characteristics showed similar lateralities of the measured eyes ($P = 1.00$) and keratometry values ($P = .67$) for both groups. The group of patients with ND, however, contained a significantly higher percentage of female ($P < .01$) and younger subjects ($P = .04$) than those in the group of

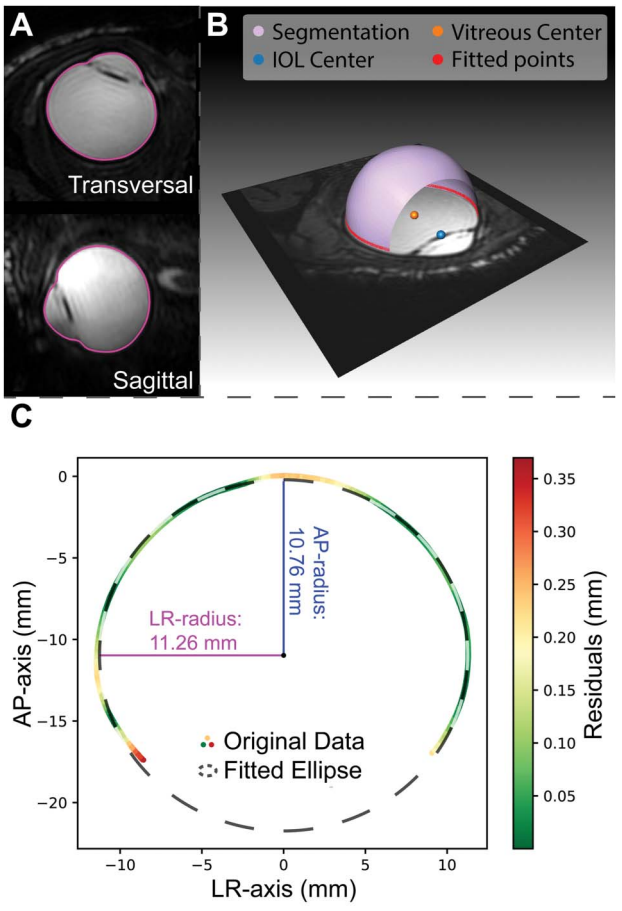

Figure 3. Example of the determination of the retinal shape using the 3DT2 scan. *A*: The segmented boundary of the vitreous body (*purple*). *B*: The segmented vitreous body (*light purple*), the IOL center (*blue*), the vitreous center (*orange*), and the horizontal slice selected for ellipse fitting (*red*). *C*: The ellipse fitted to the retinal surface for 1 subject (*dashed black line*) and the original data that were fitted. The color of the data depicts the fitting residuals at each datapoint. AP = anterior–posterior; LR = left–right.

Table 1. Demographic Characteristics.

	Patients with ND	Pseudophakic controls	*P* value
Subjects, n	37	25	
Female sex (%)	86.5	48.0	<.01*
Laterality (% right)	43.2	44.0	1.00
Age (y)			
Mean ± SD	66.1 ± 8.1	70.4 ± 8.1	.04*
Km, corneal (D)			
Mean ± SD	44.0 ± 1.5	44.1 ± 1.3	.67
ACD (internal)[a] (mm)			
Mean ± SD	4.2 ± 0.4	4.3 ± 0.2	.32
AL (mm)			
Mean ± SD	23.3 ± 1.0	24.0 ± 1.5	.04*

ACD = anterior chamber depth; AL = axial length; Km = mean keratometry; ND = negative dysphotopsia

*Statistically significant

[a]ACD was measured manually on 3 different Scheimpflug images and averaged. This measurement was not possible for 2 patients with ND and 1 pseudophakic control.

The groups were similar in all parameters except for a higher percentage of female subjects in the group of patients with ND and slightly longer eyes in the group of pseudophakic controls

pseudophakic controls (Table 1). The mean ± SD internal ACD was 4.2 ± 0.4 mm for the patients with ND and 4.3 ± 0.2 mm for the pseudophakic controls. These ACDs showed no statistically significant difference in variation (P = .14, Levene test) or in mean value between both groups (P = .32). The corresponding axial lengths were, on average, 23.3 ± 1.0 mm for the patients with ND and 24.0 ± 1.5 mm for the pseudophakic controls, with an unequal variation (P = .04, Levene test) and statistically significant difference (P = .04) between both groups (Table 1).

All patients completed the full MRI protocol; however, the faster scan with a slightly lower resolution that required no blinking was added for 2 subjects because they had difficulty to adhere to the cued-blinking instructions (Figure 1, A and B). The IOL could be clearly discriminated from the surrounding structures on both T1- and T2-weighted images. On T1-weighted images, the hydrophobic IOLs appeared hypointense, whereas the hydrophilic IOL types appeared hyperintense (Figure 1, A and C). On T2-weighted images, all IOLs appeared hypointense compared with the images of vitreous (Figure 1, B). The 3DT1 scan was of insufficient quality to determine the iris and/or IOL location in 3 pseudophakic controls, and the automated quantification of the retinal shape based on the 3DT2 required manual correction in 4 patients with ND and 2 pseudophakic controls because of movement artifacts (Figure 1, D and E). All other ocular measurements were completed successfully. On the tomography images of 2 patients with ND and 1 control, however, the IOL could not be visualized, preventing the determination of the iris–IOL distance.

The mean distance between the iris and the IOL, as determined with anterior chamber tomography, was 1.1 ± 0.2 mm in both patients with ND and pseudophakic controls and did not differ statistically significantly between both groups (P = .75) (Figure 4, A). The displacement of the IOL center about the pupil center, as determined on the 3DT1 MRI scan, was, on average, 0.0 ± 0.2 mm in the horizontal plane and 0.0 ± 0.3 mm in the vertical plane for the patients with ND. For the pseudophakic controls, this displacement was 0.1 ± 0.3 mm horizontally and 0.0 ± 0.3 mm vertically. No statistically significant differences in IOL alignment were apparent in either horizontal (P = .36) or vertical (P = .71) direction (Table 2 and Figure 4, B). The reproducibility analysis of the horizontal IOL alignment showed a small nonsignificant bias of 0.01 mm, with an SD of 0.23 mm between both analyses.

The mean tilt of the IOL about the iris, as obtained from the T1-weighted images, was 0.0 ± 0.5 degrees horizontally and 0.3 ± 1.3 degrees vertically for the patients with ND. For the pseudophakic controls, this tilt was 0.0 ± 0.3 degrees horizontally and 0.5 ± 0.9 degrees vertically. Neither in the horizontal (P = .70) nor vertical (P = .54) direction did these findings differ statistically significantly between both groups.

The determined retinal shapes, quantified by the radii of the fitted ellipses, showed a significant correlation with the axial length, with all P values being <.01 (Figure 5). For the patients

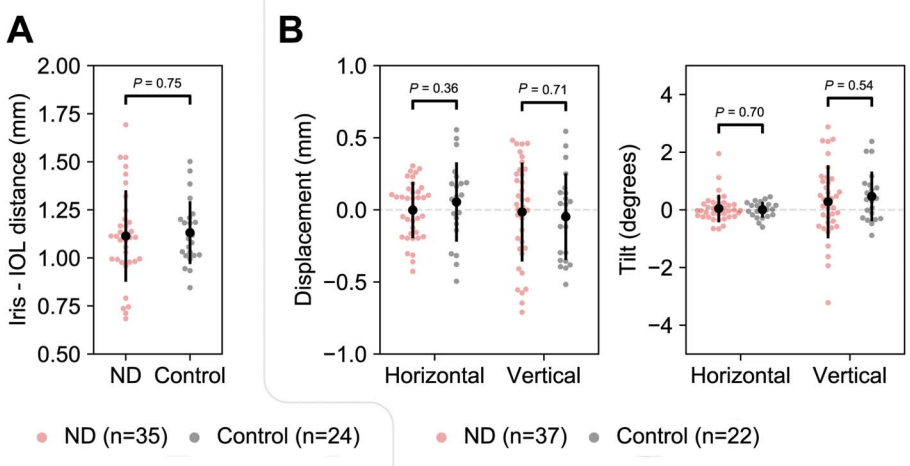

Figure 4. Evaluation of the geometric relation between the iris and IOL. *A*: Distance between the iris and the IOL as measured with anterior segment tomography for patients with ND (*red*) and pseudophakic controls (*gray*) together with the groupwise means (*black dots*) and SDs (*vertical black lines*). *B*: Displacement of the IOL center about the pupil center and tilt of the IOL about the iris as measured with ocular MRI. Positive values indicate a displacement or tilt toward the temporal or superior side. ND = negative dysphotopsia.

Table 2. Evaluation of the Geometric Relation Between the Iris and IOL Using the 3DT1 MR Images.

	Patients with ND	Pseudophakic controls	*P* value
Included subjects (n)	37	22	
IOL displacement, horizontal (mm)			
Mean ± SD	0.0 ± 0.2	0.1 ± 0.3	.36
IOL displacement, vertical (mm)			
Mean ± SD	0.0 ± 0.3	0.0 ± 0.3	.71
IOL tilt, horizontal (°)			
Mean ± SD	0.0 ± 0.5	0.0 ± 0.3	.70
IOL tilt, vertical (°)			
Mean ± SD	0.3 ± 1.3	0.5 ± 0.9	.54

MR = magnetic resonance; ND = negative dysphotopsia
Displacement of the IOL is reported about the pupil center and the IOL tilt relative to the iris plane. Positive values indicate a displacement or tilt toward the temporal or superior side. No statistically significant differences were found between the groups.

with ND, the mean radius was 10.4 ± 0.6 mm in the AP direction and 11.7 ± 0.5 mm in the LR direction. For the controls, these mean radii were 10.7 ± 0.8 mm and 11.8 ± 0.6 mm, respectively (Table 3 and Figure 5). When the axial length was taken as a covariate, no statistically significant differences were found between the LR radii (P = .10) or the AP radii (P = .56) of both groups.

DISCUSSION

The exact mechanism behind ND has been unknown since its original description in 2000, and even though various studies on the origin of this complaint have been performed, many potential factors of influence are still to be evaluated in clinical studies.[1] In this study, we compared the in-the-bag position of the IOL and the retinal shape between a group of patients with ND and a group of pseudophakic controls. Using these groups, we were not able to identify statistically significant differences between patients with and without ND in either the in-the-bag position of the IOL or the retinal shape.

Both groups showed similar demographic characteristics, except for a significantly higher percentage of female subjects (P < .01), a significantly younger age (P = .04), and a small, but significantly shorter axial length (P = .04) in the patients with ND. Both the younger age and shorter axial lengths of patients with ND were also reported in the study by Makhotkina et al.[3] In a different study, they also reported a higher percentage of females than males within their evaluated treatment group.[8] Furthermore, a relation might exist between the percentage of females and the shorter axial length, but the nature of such a relation cannot be inferred from the current data.[29]

The axial position of the IOL was similar in both groups, with an approximately equal distance between the iris and the IOL (Figure 4, A). In addition, only small variations were seen in both horizontal and vertical displacement of the IOL about the pupil center in both groups, with all displacements being less than 0.8 mm (Table 2 and Figure 4, B). Furthermore, the tilt of the IOL about the iris showed minor within-groups variations for horizontal tilts, with all tilts less than 2.0 degrees, and a slightly larger variation in the vertical direction, with all tilts less than 4.0 degrees (Table 2 and Figure 4, B). Overall, the variation of these measurements was also comparable between both groups, not resulting in statistically significant differences with P values of 0.6 and higher (Table 2 and Figure 4, A and B). The larger variation in vertical direction might be because of haptic design and haptic orientation, but more knowledge on the exact IOL design is required for a more in-depth analysis of this difference. In an earlier study, largely based on the same group of subjects, it was found that the iris of patients with ND showed a significantly larger tilt toward the temporal side of the head compared with the iris of pseudophakic controls.[18] Because the result of this study showed that the IOL is aligned with the iris, it strengthens the idea that the complete eye of patients with ND is rotated more toward the temporal side of the head instead of solely the iris, which is in line with the thought that patients with ND might have a larger angle between the optical and visual axis.[14,18]

The retinal shape, quantified by the radii of a fitted ellipse in AP and LR directions, showed comparable radii in both patients with ND and pseudophakic controls, which were, on average, larger in the LR direction in both groups (Table 3 and Figure 5). These radii correlated significantly with the axial length, which correspond to the earlier described correlations of similar measurements with refraction and of axial length with refraction.[29,30] In addition, the difference between the AP and LR radii correspond to a positive asphericity of the retinal surface, which is in agreement with the study by Atchison et al.[26,31] The lack of difference between both groups indicates that it is unlikely that ND is primarily caused by a difference in retinal shape. It is, furthermore, noteworthy that the width of the eye was similar in both groups because this width,

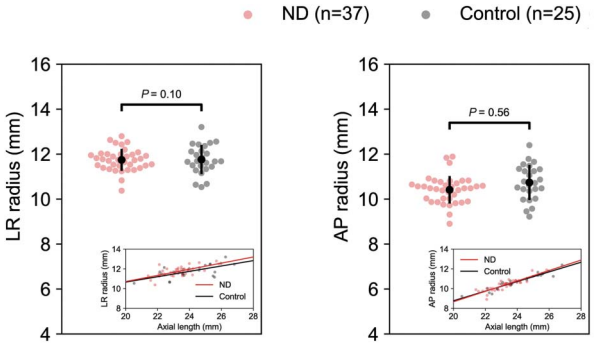

Figure 5. Evaluation of the retinal shape. The shape is quantified by radii in the LR and AP directions for patients with ND (*red*) and pseudophakic controls (*gray*) together with the groupwise means (*black dots*) and SDs (*vertical black lines*). In addition, the insets show the correlations between these radii and the axial length. All correlations are statistically significant (P < .01), with Pearson r values of ≥0.65 for the LR radius and ≥0.88 for the AP radius. When the axial length was taken as a covariate, no statistically significant differences were found between the LR radii (P = .10) or the AP radii (P = .56) of both groups. AP = anterior–posterior; LR = left–right; ND = negative dysphotopsia.

Table 3. Evaluation of Retinal Shape.

	Patients with ND	Pseudophakic controls	*P* value
Included subjects (n)	37	25	
Fitted ellipse, AP radius (mm)			
Mean ± SD	10.4 ± 0.6	10.7 ± 0.8	.10
Fitted ellipse, LR radius (mm)			
Mean ± SD	11.7 ± 0.5	11.8 ± 0.6	.56

AP = anterior–posterior; LR = left–right; ND = negative dysphotopsia
The radii of the ellipse fitted to the retinal surface. No statistically significant differences were found between both groups.

together with the location of the ora serrata, will affect the peripheral visual field eccentricities from which light is perceived on the functional retina and how it is perceived. However, the location of the ora serrata cannot be obtained from the MR images, so this cannot yet be fully assessed.

Although this study did not reveal differences in IOL position or retinal shape between patients with and without ND, this absence of differences could be potentially because of study limitations such as the limited resolution of the MRI or the number of evaluated subjects. However, the reproducibility of the MRI measurement shows that, given the size of our cohort, the mean horizontal IOL displacement of patients with ND was less than 0.1 mm (P = .05), making it unlikely to be the primary cause of ND. In addition, an earlier study showed a high, subpixel, reproducibility of 0.1 mm in the retinal shape description using a similar high-resolution MRI protocol.[24] The observed high, more than 2 mm, intersubject variation in radii of the eye in both groups are, therefore, not because of a measurement uncertainty but caused by the natural variation in eye shape. Given the similar variation in retinal shape within both groups, this shape is, therefore, unlikely to be directly linked to ND. The intersubject variation of the retinal shape will, however, be of interest for future studies using ray-tracing simulations to assess peripheral vision and related complaints such as ND. For these assessments, a more accurate retinal description will allow for a more accurate determination of whether the peripheral shadow would be sufficiently in focus to be perceived by the subject or not. However, future studies should fully personalize eye models to enable patient-specific ray-tracing analyses for these assessments.

These patient-specific ray-tracing analyses could, furthermore, aid in linking these factors with the earlier described differences in the anterior chamber configuration of patients with ND, such as an increased angle κ.[18] In addition, these analyses can potentially provide insight into the exact mechanism of certain reported treatments, including, for example, placement of a secondary sulcus IOL, reverse optic capture, and various types of IOL exchange, and link them to the ocular anatomy.[8–13] Furthermore, they could include the proposed optical effects caused by the lens capsule, although this should not exclude clinical measurements confirming their presence in the ND population.[14,16] Because MRI, computed tomography, and ultrasound are generally not sensitive to these optical changes of the tissue, an optical imaging modality, capable of assessing the edge of the IOL, is probably required.

In this study, we used high-resolution MR images to show that the alignment of the in-the-bag IOL and its tilt about the iris and the retinal shape of patients with ND were not statistically significantly different from the general pseudophakic population. Given the wide distribution of retinal shapes, however, the retinal shape could still be an important factor in a multifactorial origin of ND and should, therefore, not be ignored.

WHAT WAS KNOWN

- Negative dysphotopsia (ND) can theoretically be caused by many factors such as a small pupil size, a large angle κ, or an optical effect of the capsular bag.
- There are differences in anterior eye segment configuration between pseudophakic eyes with and without ND.

WHAT THIS PAPER ADDS

- There were no statistically significant differences in the in-the-bag IOL positioning or retinal shape between eyes with and without ND.
- There was a large variation in peripheral retinal shape, which is relevant for further peripheral vision research.

REFERENCES

1. Davison JA. Positive and negative dysphotopsia in patients with acrylic intraocular lenses. J Cataract Refract Surg 2000;26:1346–1355
2. Geneva II, Henderson BA. The complexities of negative dysphotopsia. Asia Pac J Ophthalmol (Phila) 2017;6:364–371
3. Makhotkina NY, Nijkamp MD, Berendschot T, van den Borne B, Nuijts R. Effect of active evaluation on the detection of negative dysphotopsia after sequential cataract surgery: discrepancy between incidences of unsolicited and solicited complaints. Acta Ophthalmol 2018;96:81–87
4. Osher RH. Negative dysphotopsia: long-term study and possible explanation for transient symptoms. J Cataract Refract Surg 2008;34:1699–1707
5. Henderson BA, Geneva II. Negative dysphotopsia: a perfect storm. J Cataract Refract Surg 2015;41:2291–2312
6. Cooke DL, Kasko S, Platt LO. Resolution of negative dysphotopsia after laser anterior capsulotomy. J Cataract Refract Surg 2013;39:1107–1109
7. Folden DV. Neodymium:YAG laser anterior capsulectomy: surgical option in the management of negative dysphotopsia. J Cataract Refract Surg 2013; 39:1110–1115
8. Makhotkina NY, Berendschot TT, Beckers HJ, Nuijts RM. Treatment of negative dysphotopsia with supplementary implantation of a sulcus-fixated intraocular lens. Graefes Arch Clin Exp Ophthalmol 2015;253:973–977
9. Masket S, Fram NR, Cho A, Park I, Pham D. Surgical management of negative dysphotopsia. J Cataract Refract Surg 2018;44:6–16
10. Masket S, Fram NR. Pseudophakic negative dysphotopsia: surgical management and new theory of etiology. J Cataract Refract Surg 2011;37:1199–1207
11. Vamosi P, Csakany B, Nemeth J. Intraocular lens exchange in patients with negative dysphotopsia symptoms. J Cataract Refract Surg 2010;36:418–424
12. Taubenslag KJ, Groos EB, Parker MG, Ewald MD, Pilkinton RD. Successful treatment of negative dysphotopsia with in-the-bag intraocular lens exchange using a wide ovoid IOL. J Cataract Refract Surg 2016;42:336–337
13. Burke TR, Benjamin L. Sulcus-fixated intraocular lens implantation for the management of negative dysphotopsia. J Cataract Refract Surg 2014;40:1469–1472
14. Holladay JT, Simpson MJ. Negative dysphotopsia: causes and rationale for prevention and treatment. J Cataract Refract Surg 2017;43:263–275
15. Holladay JT, Zhao H, Reisin CR. Negative dysphotopsia: the enigmatic penumbra. J Cataract Refract Surg 2012;38:1251–1265

16. Hong X, Liu Y, Karakelle M, Masket S, Fram NR. Ray-tracing optical modeling of negative dysphotopsia. J Biomed Opt 2011;16:125001
17. Simpson MJ. Mini-review: far peripheral vision. Vision Res 2017;140: 96–105
18. van Vught L, Luyten GPM, Beenakker JM. Distinct differences in anterior chamber configuration and peripheral aberrations in negative dysphotopsia. J Cataract Refract Surg 2020;46:1007–1015
19. Lemke AJ, Alai-Omid M, Hengst SA, Kazi I, Felix R. Eye imaging with a 3.0-T MRI using a surface coil—a study on volunteers and initial patients with uveal melanoma. Eur Radiol 2006;16:1084–1089
20. de Graaf P, Goricke S, Rodjan F, Galluzzi P, Maeder P, Castelijns JA, Brisse HJ; European Retinoblastoma Imaging Collaboration (ERIC). Guidelines for imaging retinoblastoma: imaging principles and MRI standardization. Pediatr Radiol 2012;42:2–14
21. Richdale K, Wassenaar P, Teal Bluestein K, Abduljalil A, Christoforidis JA, Lanz T, Knopp MV, Schmalbrock P. 7 Tesla MR imaging of the human eye in vivo. J Magn Reson Imaging 2009;30:924–932
22. Beenakker JW, van Rijn GA, Luyten GP, Webb AG. High-resolution MRI of uveal melanoma using a microcoil phased array at 7 T. NMR Biomed 2013;26:1864–1869
23. Berkowitz BA, McDonald C, Ito Y, Tofts PS, Latif Z, Gross J. Measuring the human retinal oxygenation response to a hyperoxic challenge using MRI: eliminating blinking artifacts and demonstrating proof of concept. Magn Reson Med 2001;46:412–416
24. Beenakker JW, Shamonin DP, Webb AG, Luyten GP, Stoel BC. Automated retinal topographic maps measured with magnetic resonance imaging. Invest Ophthalmol Vis Sci 2015;56:1033–1039
25. Atchison DA, Jones CE, Schmid KL, Pritchard N, Pope JM, Strugnell WE, Riley RA. Eye shape in emmetropia and myopia. Invest Ophthalmol Vis Sci 2004;45:3380–3386
26. Atchison DA, Pritchard N, Schmid KL, Scott DH, Jones CE, Pope JM. Shape of the retinal surface in emmetropia and myopia. Invest Ophthalmol Vis Sci 2005;46:2698–2707
27. Beenakker JW, Ferreira TA, Soemarwoto KP, Genders SW, Teeuwisse WM, Webb AG, Luyten GPM. Clinical evaluation of ultra-high-field MRI for three-dimensional visualisation of tumour size in uveal melanoma patients, with direct relevance to treatment planning. MAGMA 2016;29:571–577
28. Savini G, Olsen T, Carbonara C, Pazzaglia S, Barboni P, Carbonelli M, Hoffer KJ. Anterior chamber depth measurement in pseudophakic eyes: a comparison of Pentacam and ultrasound. J Refract Surg 2010;26:341–347
29. Zocher MT, Rozema JJ, Oertel N, Dawczynski J, Wiedemann P, Rauscher FG; EVICR.net. Biometry and visual function of a healthy cohort in Leipzig, Germany. BMC Ophthalmol 2016;16:79
30. Pope JM, Verkicharla PK, Sepehrband F, Suheimat M, Schmid KL, Atchison DA. Three-dimensional MRI study of the relationship between eye dimensions, retinal shape and myopia. Biomed Opt Express 2017;8: 2386–2395
31. Atchison DA, Smith G. Chapter 2: refracting components: cornea and lens. In: Atchison DA, Smith G, eds. Optics of the Human Eye. Edinburgh, UK: Butterworth-Heinemann; 2000:11–20

OTHER CITED MATERIAL

A. Jones E, Oliphant T, Peterson P. SciPy: open source scientific tools for Python. 2001

Disclosures: *L. van Vught, G.P.M. Luyten, and J.-W.M. Beenakker have a patent pending on intraocular lens design. No other disclosures were reported.*

First author:
Luc van Vught, BSc

Department of Ophthalmology, Leiden University Medical Center, Leiden, the Netherlands